*36th EPS Conference on Plasma Phys. Sofia, June 29 - July 3, 2009 ECA Vol.**33E**, P-1.159 (2009)*

Multiple diagnostic data analysis of density and temperature profiles in ASDEX Upgrade

R. Fischer, A. Burckhart, N. Hicks, B. Kurzan, E. Wolfrum, ASDEX Upgrade Team

Max-Planck-Institut für Plasmaphysik, EURATOM Association, D-85748 Garching, Germany

A major challenge in nuclear fusion research is the coherent combination of measurements from heterogeneous diagnostics. Different measurement techniques for measuring the same subset of physical parameters provide complementary and redundant data for, e.g., improving the reliability of physical parameters, considering all dependencies within and between diagnostics, and resolving data inconsistencies. Coherent combination means the integration of diagnostics raw data including forward modeling instead of the combination of diagnostics results which frequently relies on cumbersome iterative procedures. The Integrated Data Analysis (IDA) approach provides a full probabilistic model including physical and statistical description of an integrated set of different diagnostics.

IDA was applied to analyse the combined data from Lithium beam (LIB), DCN interferometry, electron cyclotron emission (ECE), and Thomson scattering (TS) diagnostics at ASDEX Upgrade to obtain full electron density and temperature profiles with a temporal resolution of up to 50 μs and a spatial resolution up to 5 mm at the plasma edge. Interdependencies of profiles between different diagnostics are fully considered. IDA enables us to study the fast temporal evolution of density, temperature and pressure profiles for inter-ELM phases as well as ELM resolved [1].

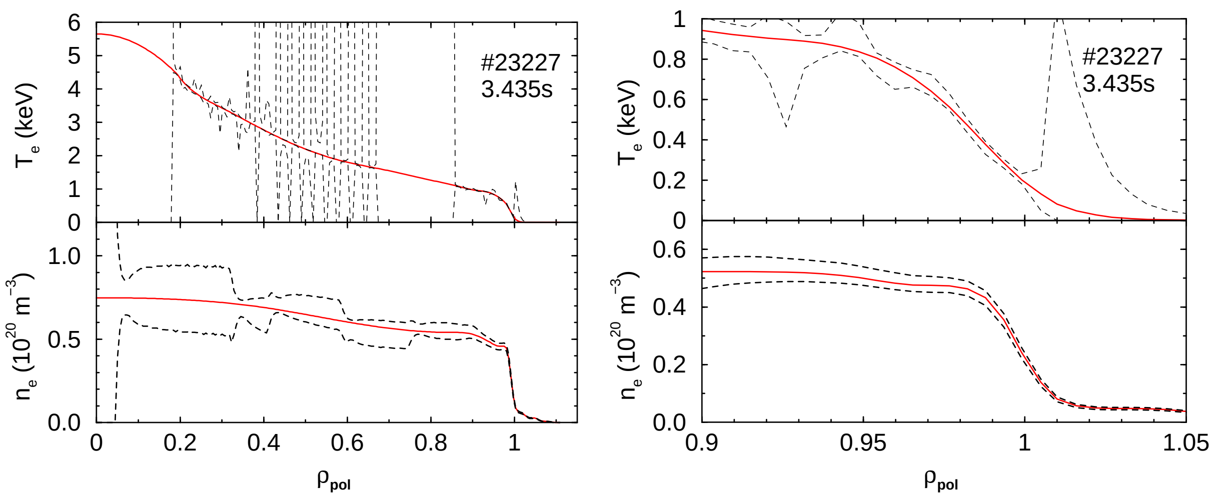

Figure 1: Temperature and density profiles with error bars as a function of normalized poloidal radius of the combined data from ECE, LIB and DCN interferometry with 1 ms temporal resolution (left: full; right: pedestal profiles)

Figure 1 shows temperature and density profiles for an H-mode discharge (#23227) obtained with the probabilistic analysis of the combined ECE, LIB and DCN interferometry data (left), and the details around the pedestal region (right). The error bar of the density profile is determined mainly by the LIB data at the pedestal and the 5 chords of the DCN interferometer where the line of sights are tangential to the flux surfaces. The error bar of the temperature profile is small at the nominal positions of the ECE channels and large where no ECE measurements exist and where the plasma is optically thin.

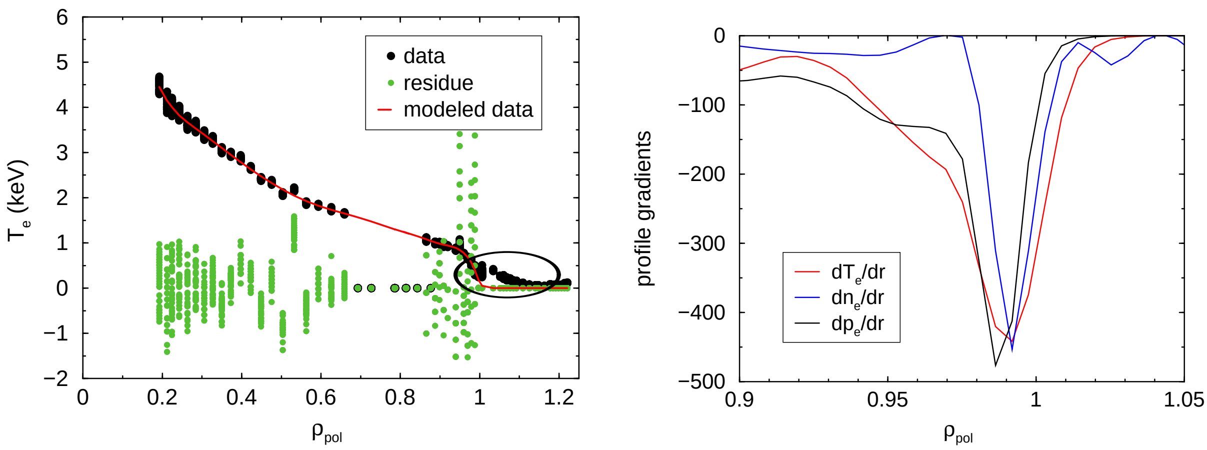

Figure 2: Left: Measured (black dots) and modeled (red line) ECE temperatures, and residuals (green dots). The ECE shine-through region is emphasized with an ellipse. Right: Gradients of electron temperature (eV/cm), density (10^{11}/cm^4), and pressure (10 Pa/cm).

Since the data of the different diagnostics are analyzed jointly, the simultaneous information about density and temperature allows to mask out the ECE channels where the plasma is optically thin (optical depth $\propto n_e T_e$) or above the cut-off density. The left panel of figure 2 shows measured and modeled ECE temperatures (keV) and the corresponding residuals weighted with the measurement uncertainties (dimensionless). For $\rho_{pol} > 0.995$ the plasma is optically thin and, therefore, the data are masked out gradually by increasing the measurement uncertainties correlated with the optical depth (for large data uncertainties the residuals become very small). IDA allows to mitigate corrupted data automatically exploiting diagnostic interdependencies.

The temperature and density profiles are parameterized with spline polynomials which easily allows to determine profile gradients. The right panel of figure 2 shows electron temperature, density, and pressure gradients. Although the temperature and density gradients peak at about the same position ($\rho_{pol} = 0.991$), the peak of the pressure gradient is shifted inwards. Again, the gradient uncertainties of T_e and p_e are large in the region where the plasma is optically thin.

Another beneficial property of the combined analysis of different diagnostics is the flexible treatment of different coordinate systems. As the diagnostics measure at different poloidal and

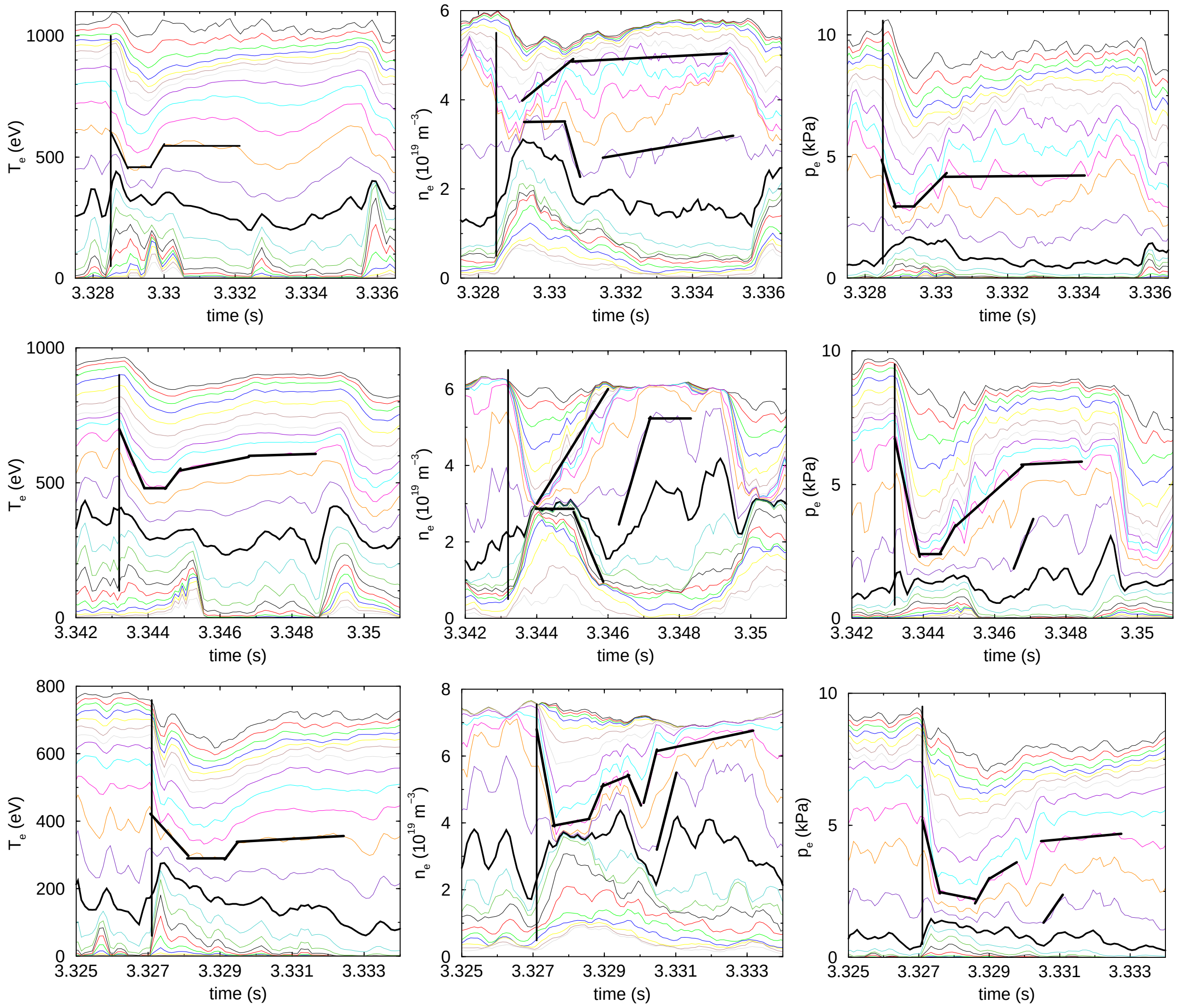

Figure 3: Temporal evolution of electron temperature, density and pressure profiles for different magnetic coordinates $\rho_{pol} = 0.88 - 1.09$ in steps of 0.01. Three different shots without (#23226, upper panel), with moderate (#23219, 4×10^{21} s^{-1}, middle panel), and large (#23225, 9×10^{21} s^{-1}, lower panel) D_2 fueling rates are shown.

toroidal positions in the plasma a common coordinate system has to be used (ρ_{pol}). Equilibrium calculations with temporal resolution of 1 ms are used to map the spatial coordinates of the LIB, DCN and TS channels and the spectral ECE channels on a common coordinate. Due to uncertainties in the determined equilibrium and due to uncertainties in the calibrated diagnostics channel positions flexibility in the mapping procedure is necessary. This flexibility is quantified by a factor which scales the coordinates of the various diagnostics. The combined analysis allows to determine these scale parameters together with the profile parameters from the data. Typical scale factors of 1.01 between TS and ECE/LIB are observed which corresponds to a shift of 5 mm at the separatrix. To reduce the uncertainty of the separatrix position additional information such as temperature constraints at the separatrix has to be provided. The following results are obtained without the TS diagnostics because the sampling frequency of about 0.1 kHz is small compared to the sampling frequencies of LIB (20 kHz), ECE (31 kHz), and DCN (10 kHz) necessary to study the temporal evolution of ELM events and inter-ELM phases.

Figure 3 shows the temporal evolution of electron temperature, density and pressure profiles between two ELM events for $\rho_{pol} = 0.88 - 1.09$ in steps of 0.01 (thick black trace at $\rho_{pol} = 1.0$). The onset of the ELM is indicated by a vertical bar. The three improved H-mode discharges have different D_2 fueling rates of 0 (#23226, upper panel), 4×10^{21} s^{-1} (#23219, middle panel), and 9×10^{21} s^{-1} (#23225, lower panel), respectively. More details about these shots can be found in [2]. Please note that the T_e profiles in the shine through region ($\rho_{pol} > 1.0$) have large uncertainties.

Although there is a natural scatter of the ELM behaviour common structures can be identified. After the ELM crash of about 0.7 ms n_e shows a plateau phase of 0.8 ms at $\rho_{pol} = 0.98 - 1.02$ and a fast recovery for $\rho_{pol} < 0.97$ within about 1.5 ms. Typically, the n_e plateau is more pronounced with gas fueling. After the fast recovery with a steepening of the n_e gradient there is a distinct difference in the n_e evolution without and with gas fueling. Without gas fueling (upper panel) the n_e gradient is continuously increasing up to 6 ms after the ELM onset. With gas fueling after the complete recovery at the pedestal top (3 ms) there is an extra steepening after about 4 ms at $\rho_{pol} = 0.98 - 1.00$. This significant difference is frequently observed and documented with ELM averaged profile evolutions of density and density gradients in [2].

The temperature profiles show a similar evolution with an ELM crash (0.7 ms), a plateau phase (0.8 ms), a fast (0.4 ms) and slow (3 ms) recovery phase. Typically, the earliest and most pronounced T_e crash is between $\rho_{pol} = 0.96 - 1.00$ where also the fastest T_e recovery appears. The pronounced extra steepening with gas fueling after about 4 ms cannot be observed in T_e.

The ELM crash is most pronounced in the pressure profiles. Please note that the $\rho_{pol} = 1.0$ trace is at about 1 kPa. The plateau region and the fast and slow recovery phases can be clearly seen for all discharges. Additionally, the extra steepening in n_e after 4 ms is also seen in p_e.

References

[1] R. Fischer, E. Wolfrum, J. Schweinzer, and the ASDEX Upgrade Team. Probabilistic lithium beam data analysis. *Plasma Phys. Control. Fusion*, 50:1–26, 2008.

[2] E. Wolfrum, A. Burckhart, R. Fischer, N. Hicks, C. Konz, B. Kurzan, B. Langer, T. Pütterich, and ASDEX Upgrade Team. Investigation of inter-ELM pedestal profiles in ASDEX Upgrade. In *Proc. of the 36th EPS Conference on Plasma Physics and Controlled Fusion*. Europ. Phys. Soc., Montreux, 2009.